Monitoring x-ray beam damage on lipid films by an integrated Brewster angle microscope/x-ray diffractometer

Stephen M. Danauskas
Department of Chemistry, The University of Chicago, Chicago, Illinois 60637, USA, The Institute for Biophysical Dynamics, The University of Chicago, Chicago, Illinois 60637, USA, and The James Franck Institute, The University of Chicago, Chicago, Illinois 60637, USA

Maria K. Ratajczak
Department of Physics, The University of Chicago, Chicago, Illinois 60637, USA, The Institute for Biophysical Dynamics, The University of Chicago, Chicago, Illinois 60637, USA, and The James Franck Institute, The University of Chicago, Chicago, Illinois 60637, USA

Yuji Ishitsuka
Department of Chemistry, The University of Chicago, Chicago, Illinois 60637, USA, The Institute for Biophysical Dynamics, The University of Chicago, Chicago, Illinois 60637, USA, and The James Franck Institute, The University of Chicago, Chicago, Illinois 60637, USA

Jeffrey Gebhardt, David Schultz, Mati Meron, and Binhua Lin
The Consortium for Advanced Radiation Sources, The University of Chicago, Chicago, Illinois 60637, USA

Ka Yee C. Lee[a)]
Department of Chemistry, The University of Chicago, Chicago, Illinois 60637, USA, The Institute for Biophysical Dynamics, The University of Chicago, Chicago, Illinois 60637, USA, and The James Franck Institute, The University of Chicago, Chicago, Illinois 60637, USA

(Received 7 May 2007; accepted 19 September 2007; published online 12 October 2007)

We describe an integrated Brewster angle microscope (BAM), Langmuir trough, and grazing incidence x-ray diffraction assembly. The integration of these three techniques allows for the direct observation of radiative beam damage to a lipid monolayer at the air-water interface. Although beam damage has been seen in x-ray measurements, it has not been directly observed *in situ* at the micron scale. Using this integrated assembly, we examined the effects of radiative beam damage on Langmuir monolayers of 1,2-dimyristoyl-*sn*-glycero-3-[phospho-L-serine] (DMPS), 1:1 DMPS:1-palmitoyl-2-oleoyl-*sn*-glycero-3-phosphocholine, and 1:1 DMPS:1,2-dioleoyl-*sn*-glycero-3-phosphocholine held at a constant surface pressure. For constant surface pressure experiments, we observed a marked decrease in the surface area of the film upon exposure to the beam due to photodissociation. For a condensed lipid film, a change in refractive index of the film was observed post-beam-exposure, indicating areas of damage. For DMPS in an oxygenated environment, the Bragg peak intensity decreased with beam exposure. In mixed monolayer systems, with saturated and unsaturated lipids, an increase in the number of small saturated lipid domains was seen as the unsaturated lipid was preferentially damaged and lost from the monolayer. We show that BAM is a highly effective technique for *in situ* observation of the effects of radiative damage at the air/water interface during a synchrotron experiment. © *2007 American Institute of Physics.*
[DOI: 10.1063/1.2796147]

I. INTRODUCTION

With the advent of highly brilliant, highly collimated synchrotron x-ray sources, the structure of biological membranes and their model systems has been probed in unprecedented detail. Unfortunately, sample damage from x-ray sources is a common problem[1–3] that needs to be taken into account. There are very few systematic studies of synchrotron x-ray damage on lipid monolayers, and to the best of our knowledge, there have been no *in situ* optical studies of x-ray damaged lipid monolayers at the micron scale.

Radiative damage of biological samples and thin films has been detected since the beginning of x-ray studies. Damage to lipid samples is primarily indirect, and believed to be mediated by hydroxyl radicals,[4,5] and enhanced by oxygen.[6] Polyunsaturated lipids with conjugated tails are easily damaged by x-ray irradiation in the presence of oxygen. In this case, a free radical cascade with a propagation step dependent on either atmospheric or dissolved oxygen appears to be the primary cause of damage.[5]

As many biological samples contain polyunsaturated lipids, it is difficult to determine the degree of damage caused by the beam as opposed to the degree of damage caused by the free radical cascade. The damage due primarily to beam exposure can be determined by studying saturated phospholipid systems, where there is no possibility of a free radical cascade. Under irradiation, hydrated dimyris-

[a)]Author to whom correspondence should be addressed. Electronic mail: kayeelee@uchicago.edu

 © 2007 American Institute of Physics

Downloaded 02 Jan 2008 to 128.135.12.127. Redistribution subject to AIP license or copyright; see http://rsi.aip.org/rsi/copyright.jsp

toylphosphatidylcholine, a fully saturated lipid, shows radiative damage. This was determined by spin trapping the radicals formed during beam exposure and detecting them via electron spin resonance spectroscopy.[2] While damage is far less in the saturated system, it still occurs and is also radical mediated.[2]

Cherezov *et al.*[2] have reported beam damage even of fully hydrated lipid samples. For the fully saturated dipalmitoylphosphatidylcholine dissolved at 50% w/w with water and placed in an x-ray capillary, the beam is found to cause irreversible damage. The footprint of the beam alters the optical properties of the lipid, darkening the area of exposure. This effect has proven to be stable for years. More fluid lipids, however, do not exhibit beam damage effects with such long term stability.[2] Thin layer chromatography of gel phase phosphatidylcholine samples postirradiation further shows that, apart from fatty acids and lysolipids,[7] lipidic polymers are formed as a result of beam damage.[2]

Synchrotron irradiation has been shown to cause damage to thin films. Richter *et al.* have demonstrated that x-ray reflectivity (XR) measurements performed at third generation synchrotron sources both reduce the thickness and increase the roughness of spin-coated multilayer thin films of poly(tert-butyl acrylate) and polystyrene.[8] This example is particularly informative, as it illustrates that changes in the film are directly related to the radiation dose and not due to secondary electron generation from the substrate. Repeated exposure of a Langmuir monolayer to a third generation synchrotron x-ray beam has also been shown to cause irreversible damage to the sample.[3] While neutron reflectivity data indicated that the adsorption of cholera toxin to a mixture of 80:20 1,2-dipalmitoyl-*sn*-glycero-3-[phospho-L-ethanolamine] (DPPE) and the ganglioside G_{M1} was complete after 3 h, XR measurements on the same system showed a continuously changing electron density profile over the course of 12 h if the XR scans were on areas previously exposed to the x-ray beam. However, XR data obtained with lateral translation of the sample to an undamaged region between individual reflectivity scans corroborated neutron reflectivity results, showing no further changes in the electron density after 3 h. The disparity between the untranslated and the translated samples is the result of cumulative x-ray damage, which is directly induced by the x-ray beam and not by a free radical chain reaction, as DPPE is fully saturated and G_{M1} is monounsaturated.

Other than the lipid beam damage work discussed above, there is a paucity of systematic studies detailing the effects of synchrotron radiation on Langmuir monolayers. Furthermore, previous studies have not linked changes observed to changes in the optical properties of the film. In the work presented here, we have used Brewster angle microscopy (BAM) to directly monitor changes in the refractive index of phospholipid monolayers during irradiation. For condensed lipid monolayers, we have observed a change in the refractive index of the film post-beam-exposure, and for mixed saturated/unsaturated lipid films, we have found an enhanced area fraction of ordered domains in the film, both in BAM and grazing incidence x-ray diffraction (GIXD) measurements, signifying that unsaturated lipids are preferentially damaged, and thus desorb from the film faster than their saturated counterparts. For the first time, concurrent measurements of BAM with GIXD allow for a physical depiction of the changes that take place during synchrotron radiation damage.

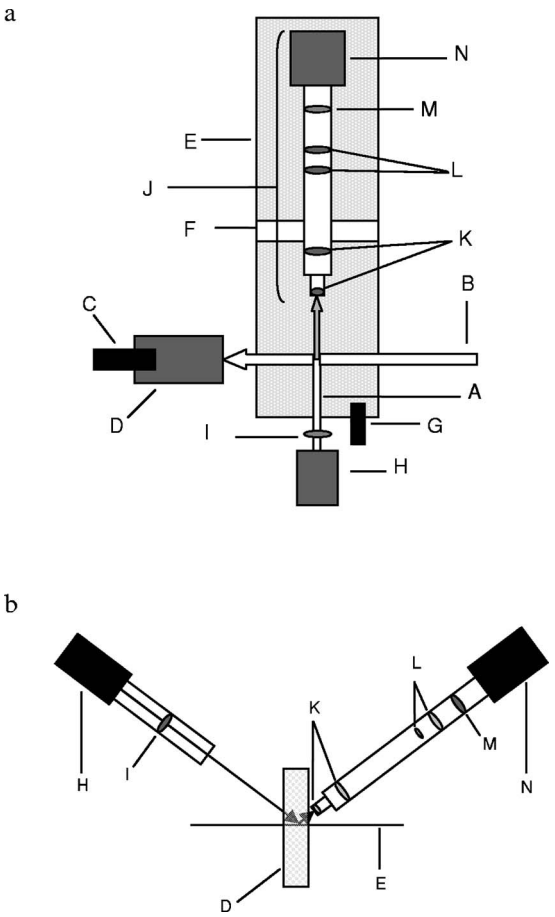

FIG. 1. (a) A schematic of the overhead view of the BAM/GIXD trough assembly. The laser beam is represented by A and the x-ray beam is represented by B. The gray portion of the laser beam denotes the path of the beam after reflection (if any) from the water surface. The laser and x-ray beams are aligned with a guide laser (C), and GIXD measurements are recorded with a linear wire detector (D). The Langmuir trough (E) has a single barrier (F), and the surface pressure is monitored using a surface pressure sensor (G). The laser (H) emits partially *p*-polarized light, which is filtered through a Glan-Thompson polarizer (I). The BAM imaging arm (J) consists of four achromatic doublet lenses arranged in two lens assemblies (K and L) in a configuration which minimizes first and second order aberrations. An analyzing polarizer (M) is positioned immediately before the CCD camera (N) to increase the contrast of the image. The BAM is attached to a linear translational stage (not shown) to allow for refocusing of the microscope during a synchrotron experiment. (b) A schematic of the side view of the BAM and GIXD detector. All labels correspond to the components labeled in (a).

II. APPARATUS

A. Principles

An overhead schematic of the Langmuir trough/BAM/GIXD assembly is shown in Fig. 1(a). For the sake of clarity, most translational stages, the trough box, and the trough lid have been omitted. Figure 1(b) shows the orientation of the BAM and GIXD detectors with respect to the water surface. The BAM is lowered over the trough, and a laser beam is

Downloaded 02 Jan 2008 to 128.135.12.127. Redistribution subject to AIP license or copyright; see http://rsi.aip.org/rsi/copyright.jsp

used to illuminate the surface. A guide laser in the plane of the x-ray beam is used to align the BAM laser with the incoming x-ray beam before the opening of the beam shutter. A linear wire detector is used to record the GIXD signal, while the surface morphology of the film is concurrently monitored by BAM.

B. Trough

A custom-built Teflon trough, controlled by a NIMA controller box (NIMA, UK) and interfaced with a computer data acquisition system written in LABVIEW, was used to run all experiments. The single barrier trough was contained in a sealable box with a Kapton window at one end to allow x-ray beam access. A surface tensiometer (NIMA, UK) mounted on the side of the trough directly opposite the barrier was used to measure the surface pressure of the film. The trough had an initial area of 322 cm^2 when completely expanded and a working volume of 320 ml. A custom made two-piece lid with a long rectangular hole in the center allowed access for the BAM. Due to the size and spatial constraints, we were unable to seal the trough during concurrent x-ray and BAM experiments. Before x-ray measurements, the trough was flushed with either high purity Ar or N_2 (99.998% pure, Airgas, Radnor, PA) until the oxygen content of the local environment was less than 1%, after which a steady stream of Ar or N_2 was used to maintain the low O_2 content. The O_2 content was measured using an AO2 O_2 sensor (McNeill International Inc., Alpharetta, GA). All experiments were performed at 23 °C unless otherwise noted. Lipid films were compressed at a rate of 0.2 cm^2/s to 25 mN/m, and the pressure was maintained by a motorized feedback loop. All temperatures reported had an error of ±2 °C.

C. X-ray instrumentation

All experiments were performed using the liquid surface spectrometer at the Chemistry and Materials Section of the Consortium for Advanced Radiation Sources (ChemMatCARS) beamline of the Advanced Photon Source at Argonne National Laboratory.[9] GIXD is a powerful technique for measuring order in two-dimensional surface films. All GIXD experiments were performed at 10 keV ($\lambda=1.24$ Å) using a linear wire detector (14 cm long with a spatial resolution of 250 μm). In a typical experiment, the sample is irradiated by x rays with wave vector $\mathbf{k}$, along the direction of the incoming beam and with a value of $k=|\mathbf{k}|=2\pi/\lambda$, at an incident angle below the critical angle for total external reflection. As a result, an evanescent wave is generated. Diffraction from the evanescent wave is observed as a function of the wave vector transfer $\mathbf{Q}$, given by $\mathbf{Q}=\mathbf{k}'-\mathbf{k}$ (where $\mathbf{k}'$ is the wave vector of the diffracted radiation), and it provides detailed information about ordering at the interface.[10] This diffraction gives rise to Bragg peaks when the three-dimensional spectrum collected by scanning over Q_{xy} (the surface parallel component of the wave vector transfer) is integrated over Q_z (the surface normal of the wave vector transfer).[10–12] The vertical slits, which control the size of the beam footprint, were opened to a total width of 0.2 mm with no aluminum absorbers in the beam path. To monitor the progression of damage, the trough was not translated during the course of the experiment. As will be shown in Sec. III, changes in the monolayer were apparent during the first x-ray scan. The GIXD instrumental parameters were the same for all experiments unless otherwise noted. In order to compare GIXD measurements, the base line intensities of all measurements within a set were scaled to be equivalent.

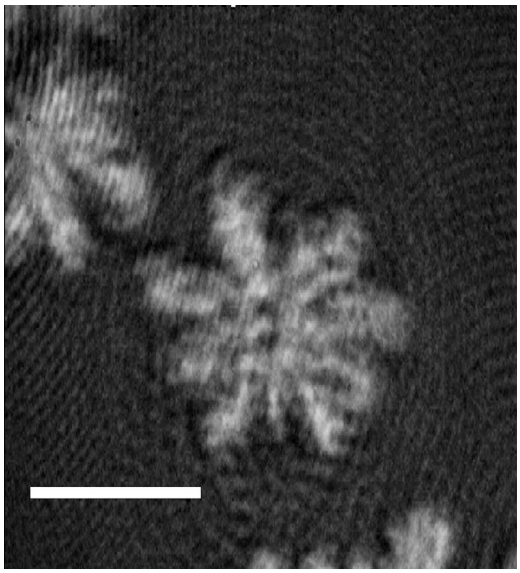

FIG. 2. Brewster angle micrographs of DMPS ($\Pi=5.7$ mN/m) on pure water at 23 °C under N_2. The film is in the liquid-expanded (dark)/condensed (bright) coexistence region; similar morphology is observed for all films. The scale bar is 50 μm in length.

D. Brewster angle microscope

Contrast in BAM is provided by the difference in orientation, thickness, and/or phase of the film at the air/water interface. BAM can detect differences of 1–2 Å in thickness,[13] so that subtle changes in the film are easily observable. At the Brewster angle for water (53.1° with respect to the surface normal), *p*-polarized light from a flat interface has no reflected beam. As the film is compressed, the difference in the refractive index increases, with the more ordered fraction of the film becoming brighter. Figure 2 shows the bright, condensed (C) 1,2-dimyristoyl-*sn*-glycero-3-[phospho-L-serine] (DMPS) domains surrounded by DMPS still in the liquid-expanded (LE) phase.

Our BAM setup is made up of two independent arms, a laser arm and an imaging arm, each mounted on a rotational stage and has a working distance of approximately 25.4 mm. The laser arm consists of a Brimrose laser with a wavelength of 532 nm and a power of 50 mW. A Glan-Thompson polarizer (Linos Photonics, Milford, MA) with a 100 000 0:1 extinction ratio, which increases the ratio of *p*-polarized light, is located immediately after the laser. This arm is mounted on a *z* stage, whereby the height of the arm can be changed remotely to account for a change in the height of the water surface. The imaging arm consists of four achromatic doublet lenses (Newport, Irvine, CA), which serve the equivalent function of the microscope objectives more commonly used in BAM.[14] The BAM lens system is composed of two sets of lens assemblies. The first lens pair [Fig. 1 (K)],

Downloaded 02 Jan 2008 to 128.135.12.127. Redistribution subject to AIP license or copyright; see http://rsi.aip.org/rsi/copyright.jsp

the objective assembly, consists of a lens with a focal length (f) of 25 mm, and a lens with an $f=150$ mm. In between each lens in an assembly is an afocal space. The second lens assembly [Fig. 1 (L) consists of a lens with $f=19$ mm and a lens with $f=125$ mm. The distance between the two lens assemblies is the sum of the focal lengths of the last lens in the first assembly and the first lens in the last assembly (a distance of 169 mm for this instrument). The distance between the camera and the second lens assembly is determined by the focal length of the final lens. In this particular instrument, the distance between the last lens and the charge coupled device (CCD) camera is 125 mm. This arrangement ensures that the image is free of first and second order optical aberrations. The microscope has a field of view of approximately 160×200 μm^2 and a nominal resolution of $3-5$ μm. A striation-free Glan-Thompson polarizer with an extinction ratio of 100 000 0:1 (Linos Photonics, Milford, MA) sits in front of the camera and is used as the analyzing polarizer. The analyzing polarizer position is set to minimize the amount of non-p-polarized light entering the camera. The imaging arm is attached to a linear translational stage which allows for focusing the microscope remotely during the course of a synchrotron experiment.

At the end of the imaging arm is a Cohu Monochrome CCD camera (Cohu, San Diego, CA). The camera outputs an interlaced signal to which text can be added by an analog overlay (model 5000A Outland Technologies, Slidell, LA). Movies of the imaged film were recorded on a Sony DV Walkman GV-D1000 NTSC (Sony Corp., Japan), and images were captured on a computer using a firewire interface. To align the BAM and the x-ray beam, the trough was filled with 320 ml of water and a guide laser was placed in the path of the incoming beam. The BAM height was then adjusted so that the paths of the lasers intersected on the water surface.

E. Lipid preparation

All lipids were purchased from Avanti Polar Lipids, Inc. (Alabaster, AL) and used without further purification. DMPS was purchased in powder form and stock solutions were prepared using a 9:1 mixture of chloroform to methanol 1,2-dioleoyl-*sn*-glycero-3-phosphocholine (DOPC) and 1-palmitoyl-2-oleoyl-*sn*-glycro-3-phosphocholine (POPC) were purchased already dissolved in chloroform. Monolayers were deposited dropwise using a Hamilton gas tight syringe (Hamilton Company, Reno, NV) to an initial surface pressure between 2 and 13 mN/m on a pure water subphase (resistivity of ~18 MΩ cm, Millipore, Billerica, MA).

F. Image analysis

Images were captured with homebuilt software and deinterlaced using a kernel based spatial/temporal algorithm for each frame. Images were taken at 30 min intervals and the lipid domain sizes were measured using the straight line function in ImageJ (NIH, Bethesda, MD). A minimum of eight images of various portions of the monolayer were taken. Rarely, one encounters portions of the film that have a different size distribution of domains with respect to the majority of the film, where all of the domains are very small. These areas were not included in our image analysis. The aspect ratio of the images was corrected for a longitudinal distortion due to the imaging angle.

III. OPERATION AND PERFORMANCE

The central interest of this study is to determine the effect of the x-ray beam on lipid monolayer spread at the air/water interface by imaging the monolayer concurrently. As such, we have carefully chosen lipid systems that minimize the secondary problem of lipid peroxidation. DMPS is fully saturated and is not subject to attack from hydroxyl radicals. Additionally, POPC and DOPC have one and two monounsaturated tails, respectively, and are not subject to the free radical cascade, which requires resonance stability of the generated free radical, that is the primary cause of indirect radiative damage.[5,15] The saturated phospholipid monolayer should therefore allow us to view the direct effect of the beam on a solid monolayer. The unsaturated lipids, on the other hand, would allow us to explore the more complicated interaction with x rays in partially fluid mixed monolayers with disaturated lipids.

We performed a systematic GIXD study of DMPS held at a constant surface pressure of 25 mN/m on a pure water subphase under three atmospheric conditions: N_2, standard atmospheric conditions, and Ar. This allows us to examine the effect of direct radiation damage to the film under different atmospheres. At ambient temperature (~23 °C), DMPS exhibits a LE/C phase coexistence region that starts at 4 mN/m (Fig. 2) and becomes completely condensed at 23 mN/m. The experiments were therefore chosen to run at a constant pressure of 25 mN/m to avoid any change in phase of the lipid during irradiation. At 25 mN/m, DMPS features a single Bragg peak centered at 1.493 Å^{-1} in Q_{xy}.

A. DMPS under N_2

To minimize the presence of oxidative damage to the film, N_2 was used to displace O_2 from the local atmosphere. Under N_2, we observed a slight destabilization of the surface pressure under irradiation. Stability of the film was determined by monitoring the area change needed to keep the surface pressure (Π) constant. A constant decrease in surface area was observed during GIXD measurements, resulting in a 2.8% decrease in area over 35 min, during which six consecutive GIXD scans were taken. Control experiments show that a decrease in area of approximately 0.3% would be expected over the same period of time for a nonirradiated condensed DMPS film.

Upon irradiation, there was a small, but measurable, decrease in the surface pressure that we were attempting to maintain, and a corresponding decrease in surface area was observed. The film area continued to decrease until the hard limit of the experimental setup was reached. We can rule out the possibility that the observed effect was due to electronic interference between the x-ray beam and the surface balance because upon discontinuation of the beam, the surface pressure was able to recover its initial value only upon further compression of the film. The observed decrease in area upon irradiation is likely due to dissociation of DMPS into

Downloaded 02 Jan 2008 to 128.135.12.127. Redistribution subject to AIP license or copyright; see http://rsi.aip.org/rsi/copyright.jsp

smaller, more water soluble components. Unfortunately, the Bragg peak for this film was weak with respect to the background, and therefore no quantitative comparison between scans could be made.

Before irradiation, BAM showed a homogenous condensed film with point scatterers randomly distributed throughout the film. The film was completely condensed [Fig. 3(a)] at ~23 mN/m. During irradiation, the film drifted in the direction of the barrier motion as the trough motor feedback attempted to maintain a constant pressure. BAM showed areas of decreased refractive index after exposure to the x-ray beam [circled segment of the film, Figs. 3(b) and 3(c)]. These areas have not previously been seen in BAM images of DMPS at this temperature and pressure prior to beam exposure. A possible explanation for the decreased refractive index is that local heating of the sample causes a change in phase behavior near the footprint of the beam. However, this is not very likely, as results from Cherezov *et al.* demonstrate that local heating of a sample during x-ray irradiation is essentially negligible.[2]

B. DMPS under an ambient atmosphere

One of the largest concerns with respect to beam damage is the effect of oxygen on the film. At energies of 10 keV, a number of atmospheric reactions can take place. O_2 can be split into molecular oxygen, a highly reactive species, and can recombine with N_2 and O_2 to form nitrogen oxides and ozone. In addition, the 1% Ar in the atmosphere can be highly ionized.[16] In this set of experiments, the temperature of the film was lowered to ~20 °C in order to obtain a better signal-to-noise ratio for the GIXD measurement. At this lower temperature, the film was more condensed at the same surface pressure and has a larger GIXD signal. Under such an oxygenated environment, changes in the DMPS Bragg peak could be easily observed. Over the course of 47.7 min, changes in both the peak intensity and the peak area were observed [Figs. 4(a) and 4(b)]. The Bragg peak decreased from a maximum of 48 549 integrated intensity counts to 42 432 integrated intensity counts over the course of the experiment [Fig. 4(b)]. In addition, we saw a significant decrease in the average molecular area of 4.2% due to the presence of the beam [Fig. 4(c)]. Although it appears that beam damage occurs at a higher rate in an ambient environment than under nitrogen, when comparing individual scans with the same parameters between the two data sets, we find no difference in the rate of decrease in surface area.

C. DMPS under Ar

To investigate the interaction between a condensed, disaturated lipid monolayer and an easily ionizable gas, we spread a DMPS monolayer, compressed it to 25 mN/m, and purged the trough container with Ar.

Under Ar, a large change in monolayer integrity upon exposure to the beam was immediately observed. The surface pressure, held constant at 25 mN/m, began to decrease appreciably. Instantly after opening the shutter, the pressure steadily decreased from 25 to 24.5 mN/m over the span of 20 s [Fig. 5(a)] as DMPS was damaged and lost from the film. When the area, instead of the surface pressure, was held constant during irradiation, the surface pressure decreased sharply, from 25 to 7 mN/m, over 981 s, and the film underwent a phase transition to the LE/C coexistence region [Fig. 5(b)]. Presumably, the film would revert to

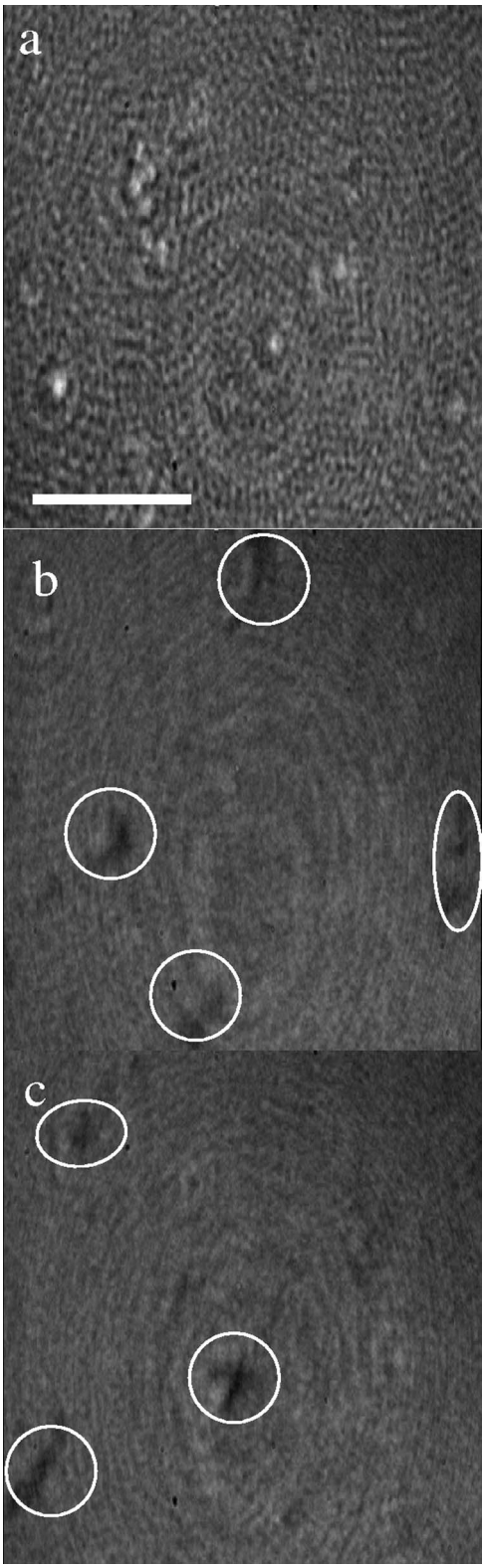

FIG. 3. BAM images of DMPS at 23 °C under N_2 at 25 mN/m (a) before and [(b) and (c)] after exposure to the beam. The circles denote areas of decreased refractive index. The scale bar is 50 μm in length.

Downloaded 02 Jan 2008 to 128.135.12.127. Redistribution subject to AIP license or copyright; see http://rsi.aip.org/rsi/copyright.jsp

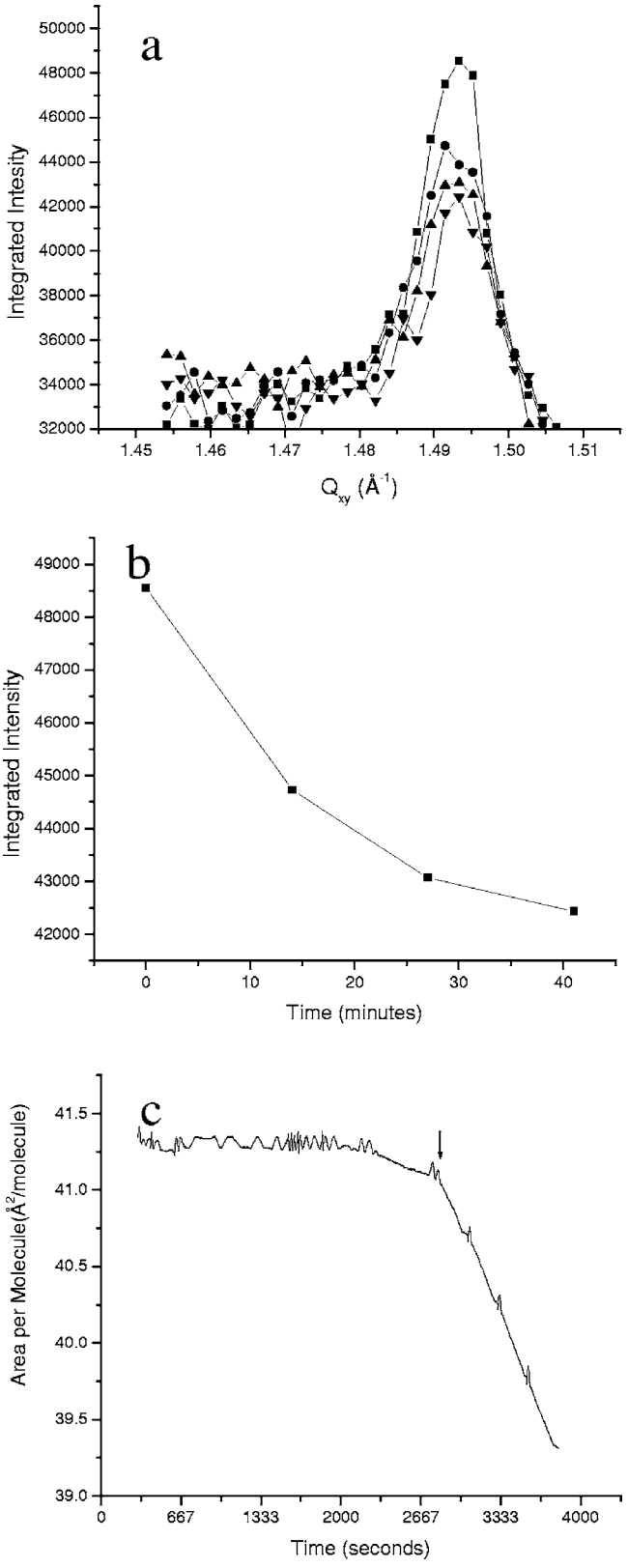

FIG. 4. (a) Bragg peaks of DMPS under ambient atmosphere. GIXD measurements correspond to t=0 (■), 14 (●), 27 (▲), and 41 (▼) min. To enhance clarity, error bars have been omitted. The error is typically within 0.5% of the measurement. (b) Decrease in GIXD maximum integrated intensity with time. (c) Change in area for the DMPS film at a constant pressure of 25 mN/m under irradiation. The arrow denotes the first time the shutter is opened for a GIXD scan.

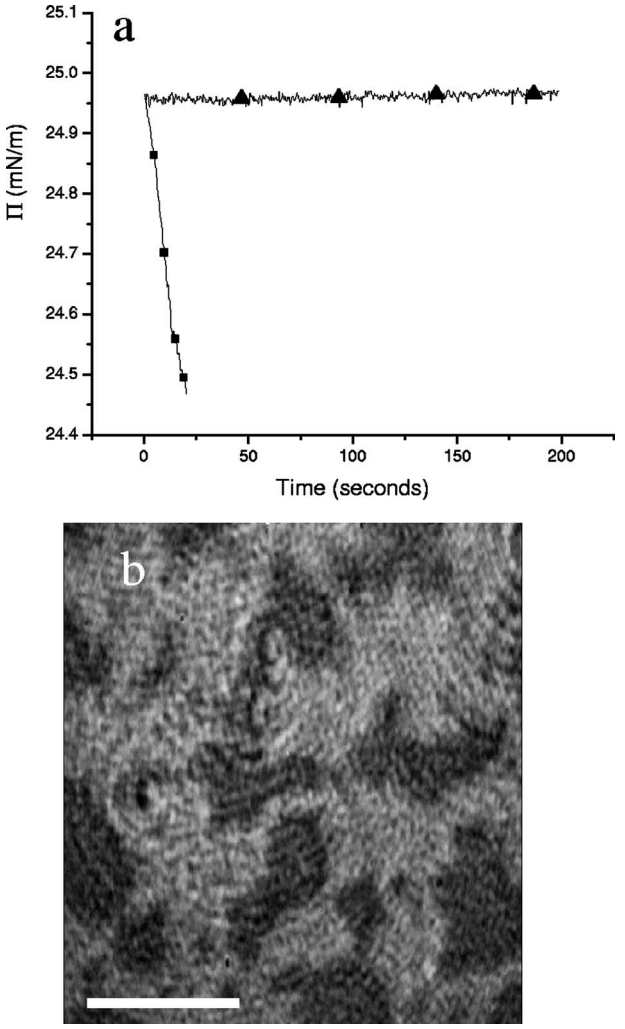

FIG. 5. (a) Change in constant surface pressure under Ar in the presence of (■) and the absence (▲) of irradiation. (b) DMPS film under Ar at constant area postirradiation: the film has reverted to the LE/C phase during irradiation. The scale bar is 50 μm in length.

the gas/LE coexistence phase if irradiated for a long enough period of time. To ensure that the observed effect was not due to monolayer leakage, the film was recompressed, upon discontinuation of the beam, to a constant surface pressure of 25 mN/m and remained stable. This indicates that the majority of the damage is due to the ionization of Ar in the local atmosphere. Ar has a large x-ray adsorption cross section of 64.22 cm^2/g at 10 keV (Ref. 17) compared to N_2 (7.13 cm^2/g), O_2 (11.36 cm^2/g), or He (0.24 cm^2/g). In addition, multiple excited states of Ar are generated in synchrotron x-ray sources with Ar^+ to Ar^{6+} observed due to k-shell ionization, Auger electron ejection, and electron shake off.[16] These highly charged ionization states, coupled with the fact that Ar does not recombine with other atmospheric gases, make it a powerful reducing agent. No GIXD data were collected for this system as the monolayer was too unstable (with Π falling rapidly) and the signal intensity was too low, owing to the large x-ray adsorption cross section of Ar. These results clearly indicate that the film, when put under an argon atmosphere, is much more susceptible to beam damage compared to being under an ambient or a nitrogen atmosphere.

Downloaded 02 Jan 2008 to 128.135.12.127. Redistribution subject to AIP license or copyright; see http://rsi.aip.org/rsi/copyright.jsp

D. Saturated/unsaturated binary lipid mixtures

Many lipid systems of considerable biological interest consist of mixtures of saturated and unsaturated lipids.[18,19] Due to the reactive double bond of the unsaturated lipid species, there is concern as to the degree of damage unsaturated lipids is subject to during x-ray irradiation. The unsaturated lipids used in this study were monounsaturated (POPC) and dimonounsaturated (DOPC), where one or both tails have a single double bond. These lipids are chosen as they are less likely to undergo hydrogen abstraction from hydroxyl radicals,[5] and any reactive intermediates formed will be short lived due to the lack of resonance stability.[15] Vesicle studies show that POPC does not undergo this type of free radical reaction even in highly oxidizing environments over 72 h, while a conjugated polyunsaturated phospholipid shows a large increase in lipid hydroperoxides over the same time period.[20] While results from vesicle studies do not necessarily translate directly to monolayers, it is nonetheless clear that it is much more difficult to peroxidize monounsaturated lipid tails compared to polyunsaturated lipid tails. It should be noted that this does not mitigate damage to the double bond from the beam itself, and free radical reactions continue to occur in irradiated films of monounsaturated lipids.[2]

DMPS and DOPC were mixed in a 1:1 molar ratio and compressed to 25 mN/m at 23 °C on a pure water subphase. Experiments involving unsaturated lipid mixtures were performed under N_2 to avoid oxidation of the lipid due to atmospheric oxygen.[21,22] Although monounsaturated films are resistant to hydroxyl radical attack, they have been shown to react with atmospheric O_2, leading to a decrease in surface pressure over time. DMPS forms condensed domains in the fluid DOPC continuum, with nucleation of the domains occurring at 19 mN/m. Under irradiation, the pressure dropped from the target pressure of 25 to 24.8 mN/m, and the area of the film decreased as material was lost from the surface. As the area decreased with increasing exposure to the beam [Fig. 4(c) is representative of this effect], nucleation of smaller condensed domains was seen [Fig. 6(b)] in the interstitial space between existing large domains [Fig. 6(a)]. These small domains increased in number as a function of beam exposure. To quantify this change in distribution, frames from the video were grabbed at 30 minute intervals and the lipid domain sizes were measured. A minimum of eight images of various portions of the monolayer were taken for each 30 min interval. Domains that were narrower than 25 pixels at their widest point were designated as small domains. At the beginning of irradiation, there was an average of 0.3 domains/frame narrower than 25 pixels. 3 h later under continuous irradiation, there was an average of 5.33 domains/frame narrower than 25 pixels. Although the image was only partially in focus due to the inherent limitations of BAM,[13,23,24] only domains smaller than 25 pixels at any location in the grabbed frame were counted as small domains. For consistency, several out-of-focus domains that were most likely less than 25 pixels in width (but appeared larger in the out-of-focus portion of the image than their actual size) were not counted. Therefore, the reported 5.33 domains/frame represents a lower limit of the small domain count.

As a control, a 1:1 DMPS:DOPC film under an inert atmosphere and without irradiation shows a slight enlargement and rounding of domains over the same time span. In areas that showed normal domain nucleation and growth, only a few small domains were seen over the course of 4.5 h. Nucleation of small, interstitial domains obtained when the film is under irradiation is likely due to a greater level of radiative damage to the unsaturated lipids over the saturated lipid. As the damaged unsaturated lipid was solubilized and lost to the subphase, the effective DMPS content in the film increased. With a large enough loss of unsaturated lipid, the film became enriched in DMPS, leading to the nucleation of small DMPS domains in the once disordered region enriched in unsaturated lipids. BAM clearly shows a difference in the film at the onset of irradiation and postirradiation [Figs. 6(a) and 6(b)].

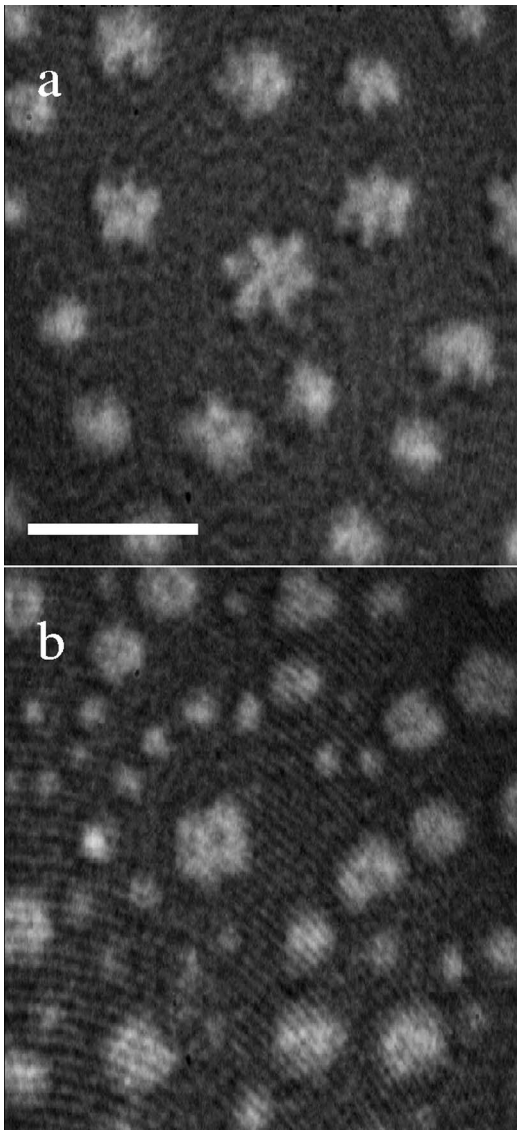

FIG. 6. 1:1 DMPS:DOPC held at a constant pressure of 25 mN/m on a pure water subphase at 23 °C under N_2 (a) at the onset of irradiation and (b) 186 min after constant irradiation. The scale bar is 50 μm in length.

We observed a similar effect in 1:1 DMPS:POPC films compressed and held at 25 mN/m at 23 °C under N_2. The pressure decreased to 24.8±0.05 mN/m under constant compression during irradiation. When the beam was removed,

Downloaded 02 Jan 2008 to 128.135.12.127. Redistribution subject to AIP license or copyright; see http://rsi.aip.org/rsi/copyright.jsp

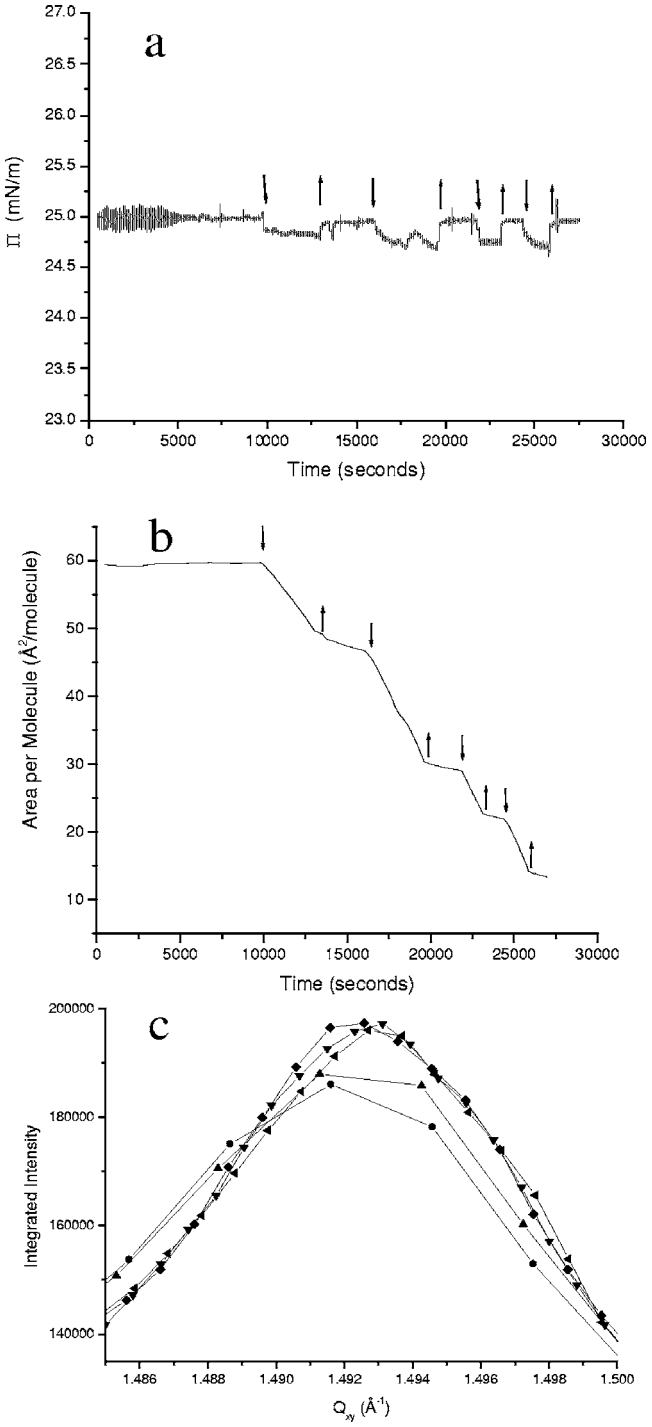

FIG. 7. (a) Change in surface pressure of 1:1 DMPS:POPC at 25 mN/m on a pure water subphase at 23 °C under N_2; downward arrows denote when the beam shutter was opened, while upward arrows denote when the beam shutter was closed. (b) The corresponding change in area upon irradiation. (c) Bragg peaks of 1:1 DMPS:POPC [t=0 min (●), 42 min (▲), 66 min (▼), 103 min (♦), and 147 min (◀)] at 25 mN/m on a pure water subphase at 23 °C under He.

the surface pressure quickly recovered to approximately 25 mN/m [Fig. 7(a): the arrows denote when the beam was present and absent]. This indicates that the damage observed is mostly caused by beam irradiation. If a free radical cascade was damaging the film, the pressure would be expected to remain unstable even after the beam was discontinued. An inspection of the change in area with respect to

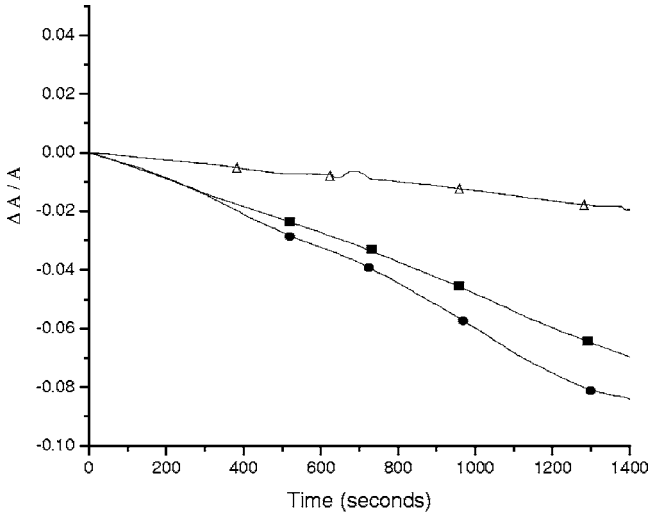

FIG. 8. Monolayer area decrease for DMPS (△), 1:1 DMPS:POPC (■), and 1:1 DMPS:DOPC (●) under irradiation. The greater the degree of unsaturation, the faster the monolayer area decreases.

time [Fig. 7(b)] verifies that the film did indeed recover its integrity when the beam was discontinued. Although there could be continuing damage to the film in the absence of the beam, this effect would seem to be minor in comparison with that due to direct beam damage. We have further obtained corroborating results from concurrent GIXD measurements, where we observed an increase in the amplitude of the GIXD scans with time, indicating that the condensed area fraction of the film increased between scans. To further explore the effects of beam damage on 1:1 DMPS:POPC mixtures, a second set of GIXD measurements was performed under similar conditions, without the BAM present. Without the spatial constraints of the BAM, we were able to substitute He for N_2 for the atmosphere in order to improve the signal-to-noise ratio. As can be seen in Fig. 7(c), there is an increase in the amplitude of the GIXD peaks as a function of beam exposure time, indicating that the area fraction occupied by the solid lipid is increasing. This further confirms that the unsaturated lipid is preferentially damaged and desorbs from the film.

A comparison of the fractional change in area between the different lipid samples (DMPS, 1:1 DMPS:DOPC, 1:1 DMPS:POPC) (Fig. 8) illustrates how the degree of beam damage is correlated to the level of lipid unsaturation. From Fig. 8, we clearly see that DMPS is least damaged by irradiation. Over the same period of time, a smaller decrease in area for the monounsaturated POPC mixed system than the dimonounsaturated DOPC mixed system has been observed. These results are in agreement with the assertion that the greater the degree of lipid unsaturation, the more susceptible the film is to radiation damage.

IV. DISCUSSION

BAM is an effective technique for observing radiative damage at the air/water interface. Using synchrotron radiation at 10 keV coupled with GIXD, we have observed changes to the film caused by radiative damage. For a saturated condensed lipid film, BAM clearly shows a change in

Downloaded 02 Jan 2008 to 128.135.12.127. Redistribution subject to AIP license or copyright; see http://rsi.aip.org/rsi/copyright.jsp

the refractive index of the film postirradiation, and a decrease in the order of the film can be observed via GIXD. Under Ar, the film exhibits an enormous amount of damage due to the large number of ionization states of Ar. BAM allows us to directly visualize the rapid loss of film integrity due to ionization. During this loss of integrity, the packing density of the film decreases and the once condensed film transitions back to a LE/C coexistence. While saturated lipids are more stable under irradiation than unsaturated lipids, we have shown that saturated lipids can nonetheless be damaged by the x-ray beam.

In mixtures of saturated and monounsaturated lipids, beam damage results in an increase in the area fraction occupied by the saturated lipid species as a function of time due to the preferential loss of the unsaturated lipid species from the film. Despite our attempt to maintain a constant pressure of 25 mN/m, we observed a slight surface pressure decrease upon irradiation. Discontinuing the beam leads to a recovery of the target surface pressure, indicating that the damage on the film is largely due to the incoming beam and not a free radical cascade.

What we have not directly addressed is the mechanism of beam damage. At 10 keV, the energy of the beam is high enough to photodissociate any bond in our lipids. The degree of damage to the film will therefore be a function of photon flux and time. Indeed, we see that if the photon flux is reduced, the change in area of the film is similarly reduced. The calculated photon flux, which takes into account the x-ray absorption of air before the air/water interface is approximately 1.5×10^{13} photons/s. Utilizing the method described by Richter *et al.*,[8] which takes into account the reflectivity of the film for a given angle, we can calculate the amount of photons absorbed by the film to be approximately 2.4×10^{10} photons/s. This relatively large absorption at an angle for which the beam experiences total external reflection can be explained by the small value for x-ray attenuation of the film at these small incident angles. From our data, we can calculate that each photon incident on the surface is responsible for damaging between ~170 molecules/s (in the case of DMPS) and ~870 molecules/s (for 1:1 DMPS:DOPC). It is likely that the damage is caused by the evanescent wave and refraction within the film, in addition to the damage caused by direct absorption. The evanescent wave effect and refraction within the film precipitate an enhancement of the electric field of the refracted beam such that it is greater than the electric field of the x-ray beam immediately before the interface.[25] In addition, high energy lipid radical intermediates may also be damaging to the film.

To the best of our knowledge, this is the first *in situ* optical study of beam damage for lipid monolayer systems. BAM used in conjunction with GIXD has allowed us to report on the morphological changes in Langmuir monolayers as a result of beam damage for saturated and unsaturated systems. We have been able to visualize the result of beam damage to mixed saturated/unsaturated systems from which we can infer the preferential damage of unsaturated lipids over saturated lipids, thus leaving the film enriched in saturated lipids. Our BAM observations corroborate results obtained by GIXD, making it possible for us to link GIXD measurements to optical properties of the film.

ACKNOWLEDGMENTS

ChemMatCARS Sector 15 is supported by the National Science Foundation/Department of Energy under Grant No. CHE-0535644. Use of the Advanced Photon Source was supported by the U. S. Department of Energy, Office of Science, Office of Basic Energy Sciences, under Contract No. DE-AC02-06CH11357. S.M.D. would like to acknowledge Kathleen Cao and Luka Pocivavsek for their assistance during the experimental run at the Advanced Photon Source. S.M.D. and Y.I. were supported in part by the University of Chicago MRSEC program of the NSF (DMR-0213748). M.R. is grateful for the support of the Burroughs Wellcome Fund. This work was partially supported by the Packard Foundation (99-1465) and the NSF (MCB-0616249).

[1] G. Cabailh, J. W. Wells, I. T. McGovern, A. R. Vearey-Roberts, A. Bushell, and D. A. Evans, Appl. Surf. Sci. **234**, 144 (2004).
[2] V. Cherezov, K. M. Riedl, and M. Caffrey, J. Synchrotron Radiat. **9**, 333 (2002).
[3] C. E. Miller, J. Majewski, K. Kjaer, M. Weygand, R. Faller, S. Satija, and T. L. Kuhl, Colloids Surf., B **40**, 159 (2005).
[4] A. W. Girotti, J. Lipid Res. **39**, 1529 (1998).
[5] G. Rosen, B. Britigan, H. Halpern, and S. Pou, *Free Radicals-Biology and Detection by Spin Trapping* (Oxford University Press, Oxford, 1999).
[6] R. Gerschman, D. L. Gilbert, S. W. Nye, P. Dwyer, and W. O. Fenn, Science **119**, 623 (1954).
[7] A. C. Cheng and M. Caffrey, Biophys. J. **70**, 2212 (1996).
[8] A. G. Richter, R. Guico, K. Shull, and J. Wang, Macromolecules **39**, 1545 (2006).
[9] B. Lin, M. Meron, J. Gebhardt, T. Graber, M. Schlossman, and P. J. Viccaro, Physica B **336**, 75 (2003).
[10] L. Scheffer, I. Solomonov, M. J. Weygand, K. Kjaer, L. Leiserowitz, and L. Addadi, Biophys. J. **88**, 3381 (2005).
[11] A. Grigoriev, O. Shpyrko, C. Steimer, P. S. Pershan, B. M. Ocko, M. Deutsch, B. Lin, M. Meron, T. Graber, and J. Gebhardt, Surf. Sci. **575**, 223 (2005).
[12] K. Y. C. Lee, J. Majewski, T. L. Kuhl, P. B. Howes, K. Kjaer, M. M. Lipp, A. J. Waring, J. A. Zasadzinski, and G. S. Smith, Biophys. J. **81**, 572 (2001).
[13] S. Henon and J. Meunier, Rev. Sci. Instrum. **62**, 936 (1991).
[14] G. Marshall, M. Dennin, and C. M. Knobler, Rev. Sci. Instrum. **69**, 3699 (1998).
[15] R. K. Brown and F. J. Kelly, in *Free Radicals*, edited by N. A. Punchard and F. J. Kelly (Oxford University Press, New York, 1996), pp. 119–131.
[16] D. A. Church, S. D. Kravis, I. A. Sellin, C. S. O, J. C. Levin, R. T. Short, M. Meron, B. M. Johnson, and K. W. Jones, Phys. Rev. A **36**, 2487 (1987).
[17] W. H. McMaster, N. K. del Grande, J. H. Mallett, and J. H. Hubbell, LLNL Report No. UCRL-50174, 1969.
[18] S. R. Shaikh, V. Cherezov, M. Caffrey, S. P. Soni, D. LoCascio, W. Stillwell, and S. R. Wassall, J. Am. Chem. Soc. **128**, 5375 (2006).
[19] S. R. Wassall, S. R. Shaikh, M. R. Brzustowicz, V. Cherezov, R. A. Siddiqui, M. Caffrey, and W. Stillwell, Macromol. Symp. **219**, 73 (2004).
[20] R. F. Jacob and R. P. Mason, J. Biol. Chem. **280**, 39380 (2005).
[21] D. J. Benvegnu and H. M. McConnell, J. Phys. Chem. **97**, 6686 (1993).
[22] B. L. Stottrup, D. S. Stevens, and S. L. Keller, Biophys. J. **88**, 269 (2005).
[23] D. Honig and D. Mobius, J. Phys. Chem. **95**, 4590 (1991).
[24] D. Honig and D. Mobius, Thin Solid Films **210**, 64 (1992).
[25] J. Wang, J. Bedzyk, and M. Caffrey, Science **258**, 775 (1992).

Downloaded 02 Jan 2008 to 128.135.12.127. Redistribution subject to AIP license or copyright; see http://rsi.aip.org/rsi/copyright.jsp